Structural Changes of the Complex between *pharaonis* Phoborhodopsin and Its Cognate Transducer upon Formation of the M Photointermediate†

Yuji Furutani,[‡,§,||] Kentaro Kamada,[‡] Yuki Sudo,[⊥] Kazumi Shimono,[⊥] Naoki Kamo,[⊥] and Hideki Kandori*[,‡,||]

Department of Materials Science and Engineering, Nagoya Institute of Technology, Showa-ku, Nagoya 466-8555, Japan, Department of Biophysics, Graduate School of Science, Kyoto University, Sakyo-ku, Kyoto 606-8502, Japan, Core Research for Evolutional Science and Technology (CREST), Japan Science and Technology Corporation, Kyoto 606-8502, Japan, and Laboratory of Biophysical Chemistry, Graduate School of Pharmaceutical Sciences, Hokkaido University, Sapporo 060-0812, Japan

Received September 28, 2004; Revised Manuscript Received November 15, 2004

ABSTRACT: *pharaonis* phoborhodopsin (*p*pR, also called *pharaonis* sensory rhodopsin II, *p*sRII) is a receptor for negative phototaxis in *Natronobacterium pharaonis*. It forms a 2:2 complex with its transducer protein, *p*HtrII, in membranes, and the association is weakened by 2 orders of magnitude in the M intermediate. Such change is believed to correspond to the transfer of the light signal to *p*HtrII. In this paper, we applied Fourier transform infrared (FTIR) spectroscopy to the active M intermediate in the absence and presence of *p*HtrII. The obtained difference FTIR spectra were surprisingly similar, notwithstanding the presence of *p*HtrII. This result strongly suggests that the transducer activation in the *p*pR−*p*HtrII system does not induce secondary structure alterations of the *p*HtrII itself. On the other hand, we found that the hydrogen bond of the OH group of Thr204 is altered in the primary K intermediate, but restored in the M intermediate. The hydrogen bond of Asn74 in *p*HtrII is strengthened in M, presumably because of the change in interaction with Tyr199 of *p*pR. These facts provided a light signaling pathway from Lys205 (retinal) of the receptor to Asn74 of the transducer through Thr204 and Tyr199. Transducer activation is likely to involve a relaxation of Thr204 in the receptor and hydrogen bonding alteration of Asn74 in the transducer, during which the helices of the transducer perform rigid-body motion without changing their secondary structures.

Rhodopsins convert light into a cellular signal or energy. Both archaeal (*1*, *2*) and visual (*3*, *4*) rhodopsins possess seven-transmembrane helical architecture, and a retinal molecule is bound to a protein through a protonated Schiff base linkage serving as a chromophore. Photoisomerization of the retinal drives protein structural changes utilized for diverse functions. Despite these similarities, there are multiple differences between archaeal and visual rhodopsins. For example, there is no homology between their amino acid sequences. Chromophore configuration is all-trans and 11-cis for archaeal and visual rhodopsins, respectively. Photoreaction is cyclic in archaeal rhodopsins, but not in visual rhodopsins.

Furthermore, the mechanisms of light-signal conversion are different between archaeal and visual rhodopsins. In a blue-light photophobic response of archaea, the seven-helix transmembrane receptor protein *pharaonis* phoborhodopsin (*p*pR,[1] also called *pharaonis* sensory rhodopsin II, *p*SRII) forms a 2:2 complex with its two-helix transmembrane transducer protein (*p*HtrII) in the unphotolyzed state (Figure 1a) (*5*). The association originates mostly from van der Waals contacts in the transmembrane region, whereas intermolecular hydrogen bonds exist between Tyr199 of *p*pR and Asn74 of *p*HtrII (Figure 1b), and between Thr189 of *p*pR and Glu43/Ser62 of *p*HtrII. Light causes transient weakening of the association by 2 orders of magnitude in the M intermediate (*6*), leading to the activation of the cytoplasmic signal cascade that is similar to the two-component system of eubacterial chemotaxis (*7*). In contrast, the seven-helix transmembrane receptor protein rhodopsin (Rh) in vertebrate vision does not associate with its soluble transducer, a G-protein transducin (Gt), in the dark. The association at the cytoplasmic surface of Rh is induced by light, and the transducer activation is coupled to a deprotonation of the retinal Schiff base in the meta-II intermediate (*8*−*10*). It is believed that the mechanism of the transducer activation for the Rh−Gt system is common among other G-protein-coupled receptors and G-proteins.

Determination of crystal structures of *p*pR (*11*, *12*) and the *p*pR−*p*HtrII complex (*5*), and bovine Rh (*13*) and Gt

† This work was supported in part by grants from Japanese Ministry of Education, Culture, Sports, Science, and Technology to H.K. and by Research Fellowships from the Japan Society for the Promotion of Science for Young Scientists to Y.F. and K.S.

* To whom correspondence should be addressed. Phone and fax: 81-52-735-5207. E-mail: kandori@nitech.ac.jp.

‡ Nagoya Institute of Technology.

§ Kyoto University.

|| Japan Science and Technology Corporation.

⊥ Hokkaido University.

[1] Abbreviations: *p*pR, *pharaonis* phoborhodopsin; *p*HtrII, truncated *pharaonis* halobacterial transducer II expressed from position 1 to 159; FTIR, Fourier transform infrared; Rh, rhodopsin; Gt, transducin; ppR$_K$, K intermediate of *p*pR; ppR$_M$, M intermediate of *p*pR; DM, *n*-dodecyl β-D-maltoside; PC, L-α-phosphatidylcholine.

10.1021/bi047893i CCC: $30.25
Published on Web 02/05/2005

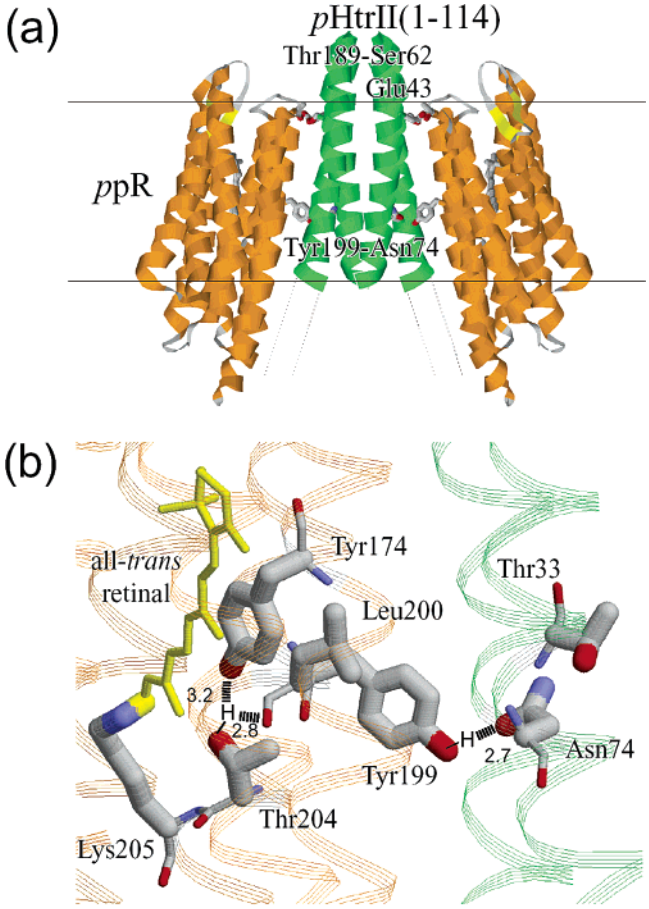

FIGURE 1: (a) X-ray crystallographic structure of the complex of *p*pR (orange) and *p*HtrII (green) (PDB entry 1H2S) (*5*). *p*pR forms a 2:2 complex with *p*HtrII in the unphotolyzed state. The association originates mostly from van der Waals contacts in the transmembrane region, whereas Tyr199 and Thr189 of *p*pR form hydrogen bonds with Asn74 and Glu43/Ser62 of *p*HtrII, respectively. (b) Details of the X-ray crystallographic structure of the *p*pR−*p*HtrII complex focusing on the key residues in this study. Dashed lines represent putative hydrogen bonds, and numbers are the distances in Å between hydrogen-bonding donors and acceptors.

(*14*), has led to a better understanding of the molecular mechanism of light signal transduction in archaea and vertebrates, respectively. However, no structures have been reported for active states of receptors or active state complexes. Receptor−transducer interactions are transient processes, and it is generally difficult to analyze such changes in protein−protein interactions at atomic resolution. Fourier transform infrared (FTIR) spectroscopy is a powerful tool for investigating protein structural changes of rhodopsins in atomic detail. We have shown that such FTIR studies can be applied not only to the intramolecular processes inside receptors but also for the intermolecular protein−protein interactions. In 1996, we first observed FTIR spectral changes in formation of a complex between activated bovine Rh and Gt (*15*). Subsequent structural analysis by use of the C-terminal peptide of the Gt α-subunit identified specific vibrational bands of the C-terminus (*16*). Similar approaches have been also reported by other groups (*17*, *18*). Recently, we have applied FTIR spectroscopy to the *p*pR−*p*HtrII complex as well. In contrast to the Rh−Gt system, *p*pR and *p*HtrII form a stable complex before the light absorption, which is advantageous for the spectral analysis. We found that the obtained spectra of the *p*pR−*p*HtrII complex for the primary K intermediate were very similar to those of *p*pR without *p*HtrII (*19*), being consistent with the crystal structure of the *p*pR−*p*HtrII complex that exhibited little structural modification of *p*pR (*5*). On the other hand, we revealed that the OH group proton of Thr204 in *p*pR is unexchangeable in D_2O, and the hydrogen bond is greatly strengthened upon retinal photoisomerization (*20*). Since this structural change takes place only in the *p*pR−*p*HtrII complex, Thr204 should play an important role in the interaction of *p*pR with *p*HtrII.

After the decay of the primary K intermediate, the M intermediate is formed in the microsecond time range. The association of the *p*pR−*p*HtrII complex is weakened by 2 orders of magnitude in the M intermediate (*6*), and the decay of the M state is delayed approximately 2-fold in the complex (*21*). These changes are somehow coupled to the activation of the transducer. Using spin labeling, Wegener et al. proposed that the outward tilt of the F-helix in the cytoplasmic region of *p*pR forces a rotational motion in *p*HtrII (*22*−*24*). According to their idea, such mechanical motion is the essence of the transducer activation (*22*). Then, the question is how the complex structure changes at the atomic level. How is the secondary structure of the transducer altered? How are the hydrogen bonding interactions between the receptor and the transducer affected? In this paper, we measured the M minus *p*pR spectra in the presence of *p*HtrII, and compared them with those in its absence. Kinetic measurements of the hydrated film samples clearly indicated formation of the complex between *p*pR and *p*HtrII. However, the obtained difference FTIR spectra were surprisingly similar between the samples with and without *p*HtrII. The similarity is prominent when the spectra for *p*pR and *p*HtrII are compared with those for bovine Rh and Gt, where significant spectral alterations are observed (*15*). This result strongly suggests that the transducer activation in the *p*pR−*p*HtrII system does not involve secondary structure alterations of the *p*HtrII itself. On the other hand, the hydrogen bonding structure of Thr204 is restored in the K-to-M transition, implying that structural changes around the retinal chromophore after photoisomerization are more extended in the M intermediate. We found that hydrogen bond of Asn74 in *p*HtrII is strengthened in the M intermediate, presumably because of the change in the interaction with Tyr199 of *p*pR. Thus, transducer activation is likely to accompany relaxation of Thr204 in the receptor and hydrogen bonding alteration of Asn74 in the transducer, during which helices of the transducer perform rigid-body motion without changing their secondary structures.

MATERIALS AND METHODS

Hydrated films of *p*pR or the *p*pR−*p*HtrII mixture were prepared as described previously (*19*, *20*), where *p*HtrII was truncated at position 159. Uniformly ^{13}C-labeled *p*pR was prepared by growing cells in standard minimal medium containing 2 g/L [^{13}C]-D-glucose (Isotec Inc.) (*19*). The N74T mutant protein of *p*HtrII was prepared as described previously (*25*). The *p*pR and *p*HtrII proteins possessing C-terminal histidine tag were expressed in *Escherichia coli*, solubilized with 1.0% *n*-dodecyl *β*-D-maltoside (DM), and purified with a Ni column. For the complex, purified *p*pR and *p*HtrII proteins were mixed in the 1:1 molar ratio, and incubated for 1 h at 4 °C. Both samples, *p*pR and the *p*pR−

*p*HtrII mixture, were then reconstituted into L-α-phosphatidylcholine (PC) liposomes (1:50 *p*pR:PC molar ratio), where DM was removed with Bio-Beads (SM-2; Bio-Rad). The PC liposomes were washed three times with a buffer at pH 7.0 (2 mM phosphate), and 90 μL of the sample was dried on a BaF_2 window with a diameter of 18 mm.

To measure the M intermediate decay kinetics in *p*pR or the *p*pR−*p*HtrII mixture, the sample was hydrated by H_2O, and placed in a cell, which was mounted in an Oxford cryostat (Optistat-DN). UV−visible spectra of the hydrated films were measured using a V-550DS (JASCO) spectrophotometer. Illumination of the sample was conducted with >400 nm light, which was supplied by a combination of a halogen−tungsten lamp (1 kW) and a long-pass filter (L42, Toshiba).

Low-temperature FTIR spectroscopy was performed as described previously (*19*, *20*, *26*, *27*). After hydration by H_2O or D_2O, the sample was placed in a cell, which was mounted in an Oxford DN-1704 cryostat placed into the Bio-Rad FTS-40 spectrometer. Illumination with >480 nm light (VY-50, Toshiba) provided by a 1 kW halogen−tungsten lamp at 250 K for 90 s converted *p*pR to pR_M. Since the pR_M completely reverted to *p*pR upon illumination with a UV light (UG-5, Melles Griot) for 90 s, as evidenced by the same (but inverted) spectral shape, the cycles of alternating illuminations with >480 nm light and UV light were repeated a number of times. The difference spectrum was calculated from the spectra constructed from 128 interferograms recorded after the illumination subtracting those recorded before the illumination. Twenty-four spectra obtained in this way were averaged for the pR_M minus *p*pR spectrum. Difference spectra at higher temperatures (270 and 290 K) were obtained by subtracting the spectra taken before the illumination from the ones taken during the illumination as described previously (*27*).

To ensure the reproducibility, we measured the FTIR spectra from two independent preparations (different expressions). In each preparation, two or three films were made and spectra were compared. All these samples produced the same results.

RESULTS

Transducer Activation in Phoborhodopsin Involves Small Structural Changes in the Peptide Backbone. First, we confirmed formation of the complex between *p*pR and *p*HtrII in the PC liposomes. Figure 2 clearly shows that the M decay kinetics is delayed 2-fold in the presence of *p*HtrII at 263 and 273 K. The same kinetic profiles were obtained for the recovery of the original state monitored at 500 nm (data not shown). These results were the same at all temperatures tested between 250 and 280 K. The 2-fold delay of the M decay is a characteristic feature of the complex between *p*pR and *p*HtrII in a DM solution as was found previously from the room-temperature flash photolysis (*21*). Therefore, this result indicates formation of the complex between *p*pR and *p*HtrII in the PC liposomes. In other words, we can safely conclude that the kinetic difference in the M decay in DM detergent is a good probe of the formation of the *p*pR−*p*HtrII complex, because such difference was also observed in membranes.

Sudo et al. showed that association between *p*pR and *p*HtrII is ∼100 times weaker in pR_M than in the unphotolyzed state (*6*, *21*), indicating that signal transduction from *p*pR to *p*HtrII involves weakening of their interaction in M. In addition to the intramolecular structural changes of *p*pR, specific change in the association between *p*pR and *p*HtrII is expected. In fact, Wegener et al. proposed a rotational motion of TM2 of *p*HtrII upon excitation of *p*pR on the basis of their spin-label experiments (*24*). How are such structural changes reflected in the vibrational bands in the FTIR spectra?

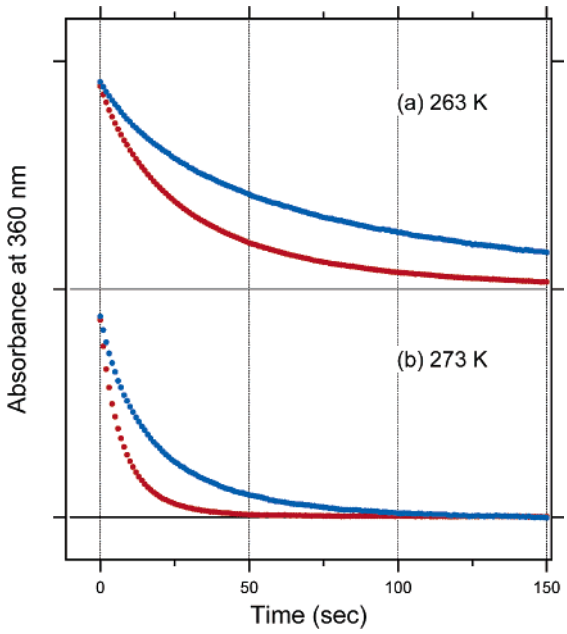

FIGURE 2: Decay kinetics of pR_M without (red curve) and with (blue curve) *p*HtrII at 263 (a) and 273 K (b). One division of the *y*-axis corresponds to 0.06 absorbance unit.

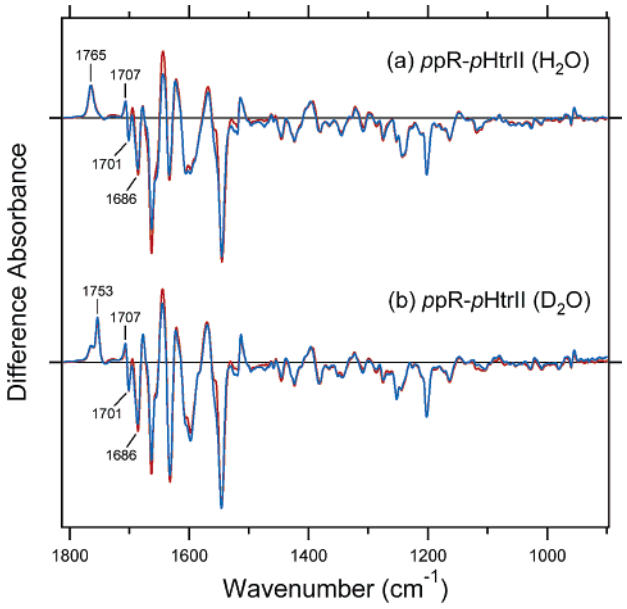

FIGURE 3: pR_M minus *p*pR infrared difference spectra without (red curve) and with (blue curve) *p*HtrII in the 1810−900 cm^{-1} region. Spectra are measured at 250 K upon hydration with H_2O (a) and D_2O (b). One division of the *y*-axis corresponds to 0.015 absorbance unit.

The pR_M minus *p*pR difference spectra in the absence (red spectra) and presence (blue spectra) of *p*HtrII are compared in H_2O (Figure 3a) and D_2O (Figure 3b). The red spectra without *p*HtrII are identical to the reported pR_M

minus *p*pR spectra (*27*, *28*), showing the protonation signal of Asp75 at 1765 and 1753 cm^{-1} in H_2O and D_2O, respectively, and D_2O-insensitive C═O stretch of Asn105 at 1707 (+)/1701 (−) cm^{-1}. Surprisingly, there are very few spectral differences in the 1800−900 cm^{-1} region between the samples with and without *p*HtrII. This fact indicates that structural changes due to the receptor−transducer interaction are much smaller than those of the receptor itself upon a transition from the resting state (*p*pR) to the active state (ppR_M). It is particularly interesting that the spectral coincidence was seen not only for the chromophore bands at 1300−1200 cm^{-1} but also for the amide I vibrations at 1700−1600 cm^{-1}. This fact also implies that structural changes of the peptide backbone are small upon activation of the transducer. This result may be in contrast to the results of the recent time-resolved FTIR studies of the *p*pR−*p*HtrII complex at 298 K, where several distinct changes were found depending on the presence of *p*HtrII (*29*). However, the difference between the two experiments does not presumably originate from the different temperatures, because similar results were obtained at 270 and 290 K, where the difference spectra were obtained by subtracting the spectra taken before the illumination from the ones taken during the illumination as described previously (*27*).

Transducer Activation in Phoborhodopsin Is Accompanied by Relaxation of Thr204 and Hydrogen Bonding Alteration of Asn74 in the Transducer. From Figure 3, it is evident that the structural changes are small in the *p*pR−*p*HtrII system compared with *p*pR itself, particularly on secondary structures. While this is true, microscopic structural changes do occur in the transducer activation processes of the *p*pR−*p*HtrII system. Such changes can be probed by highly sensitive infrared measurements, even if they are tiny. Some of such bands may be observed in panels a and b of Figure 3. Earlier, we reported the ppR_K minus *p*pR difference spectra with and without *p*HtrII, and found that complex formation influences (i) amide I vibrations that probe the peptide backbone structure of α_{II} helix and (ii) O−H stretch of Thr204 (*19*, *20*). Panels a and b of Figure 3 show the similar difference spectra with and without *p*HtrII in the 1680−1640 cm^{-1} region, implying that the former changes are reverted in ppR_M.

Figure 4 examines the O−H stretch of Thr204. Figure 4a shows the ppR_K minus *p*pR spectra in D_2O, which possesses the 3479 (−)/3369 (+) cm^{-1} bands only in the presence of *p*HtrII (*19*). Subsequent mutagenesis revealed that the bands originate from the D_2O-insensitive O−H stretching vibration of Thr204 in *p*pR (*20*). The hydrogen bond of the O−H group is strengthened to exhibit a frequency downshift by ~100 cm^{-1}, which is only observed in the presence of *p*HtrII. In contrast, the ppR_M minus *p*pR spectra do not possess the 3479 (−)/3369 (+) cm^{-1} bands (Figure 4b), indicating that the OH group of Thr204 has an identical hydrogen bond in *p*pR and ppR_M. Thus, in the *p*pR−*p*HtrII complex, the hydrogen bond of the OH group of Thr204 is strengthened upon retinal isomerization (ppR_K), while being restored upon transducer activation (ppR_M). Local structural perturbation at position 204 is relaxed at the stage of the M intermediate.

Next, we searched for the spectral difference newly appearing in ppR_M. Since the two spectra with and without *p*HtrII are very smilar as shown in panels a and b of Figure 3, we subtracted the red spectrum (without *p*HtrII) from the blue one (with *p*HtrII) in H_2O and D_2O. Consequently, such double-difference spectra provided new informative curves with reproducible bands. Panels a and b of Figure 5 show the double-difference spectra in H_2O and D_2O, respectively. We observed the 1693 (−)/1684 (+) cm^{-1} bands in the 1735−1675 cm^{-1} frequency region. If the bands originate only from the *p*pR−*p*HtrII complex, it means that the unphotolyzed (*p*pR) and ppR_M states with *p*HtrII possess vibrational bands at 1693 and 1684 cm^{-1}, respectively. However, analysis of double-difference spectra should be done carefully, because tiny differences in amplitudes may lead to apparent bands. In fact, spectral features in the 1710−1700 cm^{-1} region of panels a and b of Figure 5 presumably originate from the small difference in amplitude for the C═O stretch of Asn105 in *p*pR [1707 (+)/1701 (−) cm^{-1}] (*27*). Panels a and b of Figure 3 show the presence of a negative band at 1686 cm^{-1}, which can be ascribed to amide I vibrations. Nevertheless, the 1693 (−)/1684 (+) cm^{-1} bands were reproducible for multiple double-difference spectra, which were obtained for samples from different preparations. Therefore, we next attempted the following approach under a hypothesis that the 1693 (−)/1684 (+) cm^{-1} bands originate from the signal due to *p*HtrII.

The 1707 (+)/1701 (−) cm^{-1} bands originate from the C═O stretch of Asn105 in *p*pR (*27*). Similarly, the negative 1686 cm^{-1} band originates from vibrations in *p*pR, because it appears in the difference spectrum without *p*HtrII (red spectra of Figure 3a,b). As a result of the ^{13}C labeling of *p*pR, but not *p*HtrII, these vibrations are expected to downshift by 30−50 cm^{-1} so that vibrational bands due to *p*HtrII will appear more clearly. This was indeed the case. Red curves in panels c and d of Figure 5 correspond to the ppR_M minus *p*pR difference spectra for the ^{13}C-labeled *p*pR in H_2O and D_2O, respectively, which lack vibrational bands in the 1700−1680 cm^{-1} region because of the downshifts of the bands at 1707 (+), 1701 (−), and 1686 (−) cm^{-1} (Figure 3a,b). The ^{13}C═O stretches of Asp75 appear at 1721 and 1711 cm^{-1} in H_2O and D_2O, being shifted from 1765

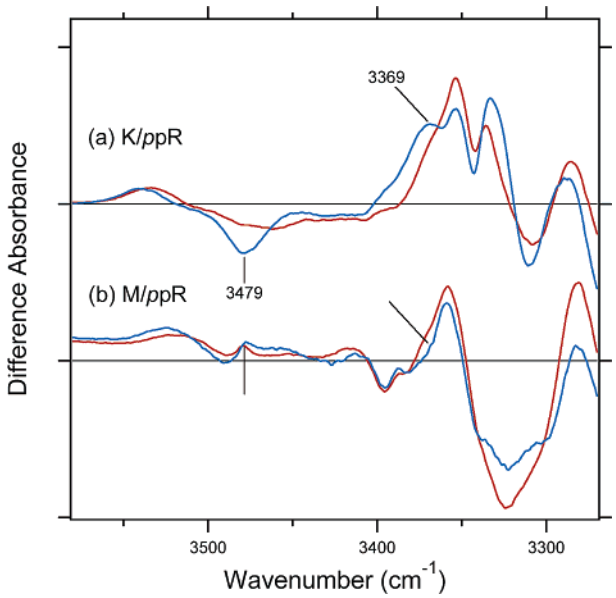

FIGURE 4: ppR_k minus *p*pR (a) and ppR_M minus *p*pR (b) infrared difference spectra without (red curve) and with (blue curve) *p*HtrII in the 3580−3270 cm^{-1} region. Spectra are measured at 77 (a) and 250 K (b) upon hydration with D_2O.

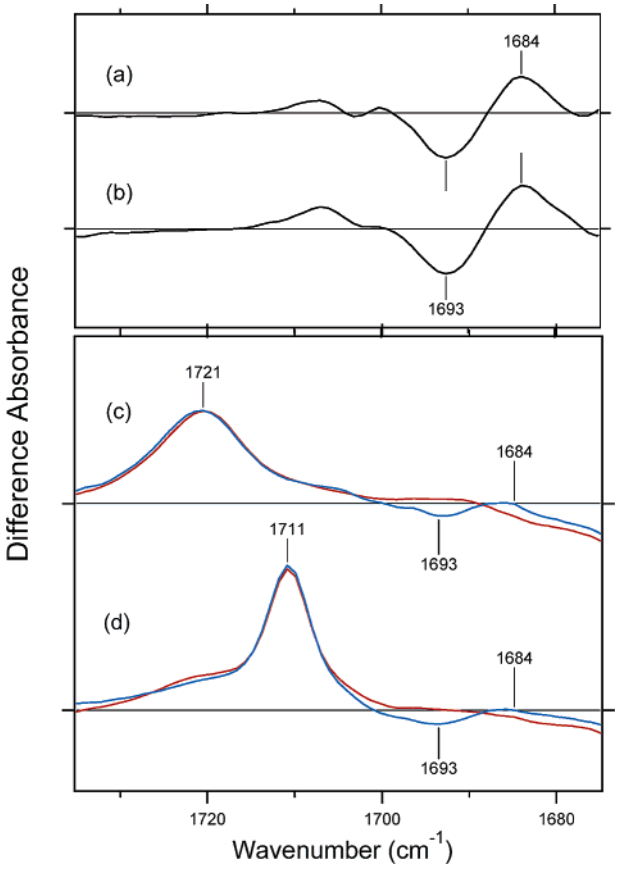

FIGURE 5: (a) Double-difference spectra obtained from the data of Figure 3a (H_2O) in the 1735−1675 cm^{-1} region, where the red curve was subtracted from the blue one. (b) Double-difference spectra obtained from the data of Figure 3b (D_2O). One division of the *y*-axis corresponds to 0.0018 absorbance unit. (c and d) ppR_M minus *p*pR infrared difference spectra for the ^{13}C-labeled *p*pR without (red curve) and with (blue curve) unlabeled *p*HtrII in the 1735−1675 cm^{-1} region. Spectra are measured at 250 K and pH 7 upon hydration with H_2O (c) and D_2O (d). One division of the *y*-axis corresponds to 0.005 absorbance unit.

and 1753 cm^{-1}, respectively. Although the presence of *p*HtrII does not affect the bands of Asp75, the clear effect of *p*HtrII can be seen in the 1700−1680 cm^{-1} region (red and blue spectra of Figure 5c,d). Panels c and d of Figure 5 show the 1693 (−)/1684 (+) cm^{-1} bands only in the presence of *p*HtrII, and the frequencies coincide with those of the double-difference spectra (Figure 5a,b). This observation strongly suggests that formation of the active ppR_M state in the complex is accompanied by a spectral downshift of a D_2O-insensitive vibrational band of *p*HtrII from 1693 to 1684 cm^{-1}.

What is the origin of the band at 1693 cm^{-1}? The frequency is characteristic of the C═O stretch of asparagine or glutamine. Amide I vibration of *p*HtrII (C═O stretch of the peptide backbone) is another candidate. These two are normally D_2O-insensitive. The X-ray structure of the *p*pR−*p*HtrII complex showed that Asn74 of *p*HtrII forms a hydrogen bond with Tyr199 of *p*pR in the middle of the membrane, while another hydrogen-bonding cluster is formed by Thr189 of *p*pR and Glu43/Ser62 of *p*HtrII at the extracellular surface (Figure 1) (*5*). Among these side chains, the C═O stretch of Asn74 is the only suitable candidate for the D_2O-insensitive 1693 cm^{-1} band. Therefore, we mutated Asn74 of *p*HtrII, and measured difference infrared spectra

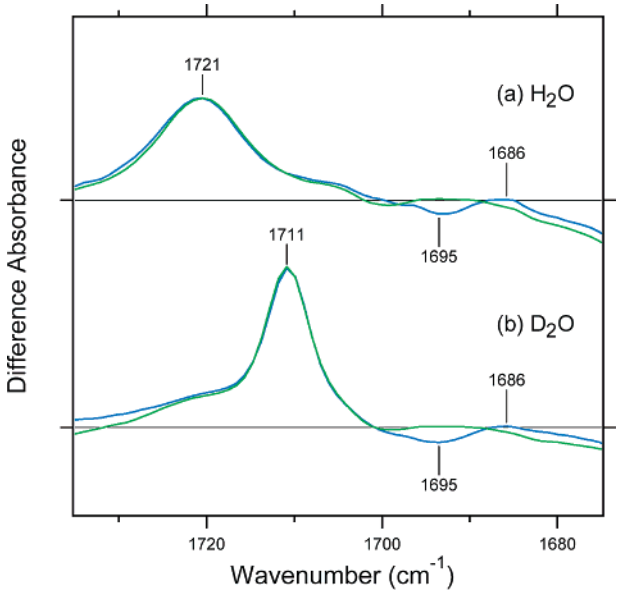

FIGURE 6: ppR_M minus *p*pR infrared difference spectra for the ^{13}C-labeled *p*pR with unlabeled wild-type (blue curve) and N74T mutant (green curve) *p*HtrII in the 1735−1675 cm^{-1} region. Spectra are measured at 250 K and pH 7 upon hydration with H_2O (a) and D_2O (b).

with ^{13}C-labeled *p*pR. In this study, we replaced Asn74 with threonine to maintain the hydrogen bonding ability of the residue at position 74. In fact, the complex between ^{13}C-labeled *p*pR and N74T mutant *p*HtrII exhibits 2-fold delay of the M decay kinetics as is the case for the wild type (Figure 2), and the ppR_M minus *p*pR spectra (data not shown) were almost identical to those of the wild type (blue curves in Figure 3a,b). Nevertheless, clear and reproducible spectral difference was observed in the 1700−1680 cm^{-1} region. Figure 6 shows that the N74T mutant of *p*HtrII lacks the 1693 (−)/1684 (+) cm^{-1} bands in both H_2O (a) and D_2O (b). Thus, we concluded that the 1693 (−)/1684 (+) cm^{-1} bands originate from the C═O stretch of Asn74.

DISCUSSION

In this paper, we measured the M minus *p*pR spectra in the presence of *p*HtrII, and compared them with those in its absence. Kinetic measurements in Figure 2 clearly indicated that the reported delayed M decay in the detergent (DM) is reproduced in the present hydrated film samples in the PC liposomes. Kinetic behavior in detergents could be significantly altered for membrane proteins. The observed behavior would be reasonable since the complex is stable even in the 1% DM detergent, being consistent with strong association ($K_d \sim 200$ nM) (*6*, *22*).

We previously reported how *p*HtrII influences the K minus *p*pR difference FTIR spectra. We observed D_2O-insensitive bands at 3479 (−)/3369 (+) cm^{-1} only in the presence of *p*HtrII (*19*), which were assigned as the O−H stretches of Thr204 in *p*pR (*20*). A large spectral downshift by 110 cm^{-1} at 77 K is unique, indicating that the hydrogen bonding interaction is greatly altered, which takes place only in the *p*pR−*p*HtrII complex. Thr204 is located near the retinal Schiff base (bound to Lys205) and the binding surface of the *p*pR−*p*HtrII complex. The results in Figure 4 indicate that the structural perturbation of Thr204 in the K intermediate is reverted in the M intermediate. Instead, a new band

appears at 1693 (−)/1684 (+) cm^{-1} in the M intermediate (Figure 5), which was identified as the C═O stretch of Asn74 of *p*HtrII (Figure 6). This observation clearly delineates the structural changes of the interaction surface of the *p*pR−*p*HtrII complex. Asn74 forms a hydrogen bond with Tyr199, which belongs to helix G as well as Thr204 and Lys205 (*5*). The OH group of Thr204 is located within hydrogen bonding distance of the side chain oxygen of Tyr174 (3.2 Å) and the peptide backbone oxygen of Leu200 (2.8 Å). Therefore, retinal photoisomerization induces a structural perturbation in the Lys205-Thr204 region observed in the K intermediate. M formation is accompanied by a relaxation of the structure at the inner face of the helix G, while the outside of helix G is perturbed at position 199. Thus, this study revealed one of the pathways in the light signal transduction, from Lys205 (retinal) of the receptor to Asn74 of the transducer through Thr204 and Tyr199.

Thr204 is unique for *p*pR. In fact, bacteriorhodopsins, halorhodopsins, and sensory rhodopsins I commonly possess Ala at this position (*30*), and only phoborhodopsins possess threonine or serine, suggesting an important role for the OH group. Thr204 and Leu200 are located between helices F and G. However, both bacteriorhodopsin and *p*pR exhibit an outward tilt of helix F in the cytoplasmic region (*22*, *23*, *31*). Therefore, Thr204 is not essential for the motion of helix F. Rather, it seems to be essential for controlling the protein−protein interaction at Tyr199.

Gordeliy et al. reported that the OH group of Tyr199 forms a hydrogen bond with the NH group of Asn74, where Asn74 is the hydrogen bonding donor (*5*). In contrast, the OH group of Tyr199 forms a hydrogen bond with the C═O group of Asn74 in the Protein Data Bank structure (1H2S), where Asn74 is the hydrogen-bonding acceptor. It may be reasonable because nitrogen and oxygen atoms of the side chain of asparagine are not easily distinguishable from X-ray analysis, where hydrogen atoms are invisible. This study identified the C═O stretch of Asn74 at 1693 cm^{-1}, being ∼10 cm^{-1} lower in frequency than that of Asn105 in *p*pR (Figure 3a,b). It is thus reasonable to suggest that the C═O group of Asn74 forms a hydrogen bond. Since there are no other hydrogen-bonding donors around the C═O group of Asn74 (*5*), it is likely that the OH group of Tyr199 forms a hydrogen bond with the C═O group of Asn74 in the complex. The C═O stretch frequency is further downshifted by 9 cm^{-1} in the M intermediate (Figure 5), indicating that the hydrogen bond has strengthened. What is the hydrogen-bonding donor? There are alternatives: (i) the OH group of Tyr199 in *p*pR or (ii) another NH or OH group such as Thr33 in *p*HtrII. In the former case, rearrangement of helices in *p*pR and *p*HtrII should take place around Tyr199 in *p*pR and Asn74 in *p*HtrII. In the latter case, switch of the hydrogen bonding interaction of Asn74 from Tyr199 of *p*pR to Thr33 of *p*HtrII may be directly correlated with the weakened complex association in M. Unfortunately, the double-difference spectra for the Y199F mutant protein were not as good as for the wild type. Further experimental efforts will lead to a better understanding of the detailed interaction at Asn74 of *p*HtrII.

One of the most surprising observations in this study was that the M minus *p*pR difference FTIR spectra were very similar with and without *p*HtrII (Figure 3a,b). The results for the *p*pR−*p*HtrII complex are in prominent contrast to the case of bovine rhodopsin (Rh) and a G-protein transducin (Gt). Upon illumination of rhodopsin, the active intermediate metarhodopsin II (meta-II) forms a complex with Gt which has GDP bound. The complex between meta-II and Gt is stable in the absence of GTP, though this does not take place under physiological conditions. We previously showed that the meta-II minus rhodopsin spectra are significantly different in the absence and presence of Gt, and the differences are prominent for amide I (1700−1600 cm^{-1}), amide II (1600−1500 cm^{-1}), and amide III (1300−1200 cm^{-1}) vibrations (*15*). Since these bands monitor vibrations of the peptide backbone, it was concluded that formation of a complex between meta-II and Gt involves peptide backbone alterations that probably originate from their interaction surface (*15*).

In the Rh−Gt system, the receptor first recognizes the terminal peptides of Gt, which must be accompanied by the secondary structure alterations. In fact, some of the changes in the peptide backbone remain in the Rh−Gt complex formed with the C-terminal peptide of the α-subunit of Gt (*16*). Molecular recognition processes in the Rh−Gt system must involve secondary structure alterations that are reflected in the amide vibrations, whereas the results presented here for the *p*pR−*p*HtrII system strongly suggest that *p*HtrII does not change the peptide backbone structure. This implies that the helices of *p*HtrII show rigid-body motions during its activation. Earlier spin-label study for a transmembrane two-helix methyl-accepting chemotaxis protein suggested that a pistonlike movement takes place (*32*). In contrast, a similar study of the *p*pR−*p*HtrII system favors rotational motion of the second helix of *p*HtrII (*24*). While these models could be different, the lack of secondary structure changes for chemotaxis proteins and *p*HtrII seems to be common during their activation. Rigid-body motions inside membrane would be transferred to the cytoplasmic end for signal transduction of light and chemicals.

ACKNOWLEDGMENT

We thank M. Sumii for her contribution in sample preparation.

REFERENCES

1. Lanyi, J. K. (2004) Bacteriorhodopsin, *Annu. Rev. Physiol. 66*, 665−688.
2. Spudich, J. L., and Luecke, H. (2002) Sensory rhodopsin II: Functional insights from structure, *Curr. Opin. Struct. Biol. 12*, 540−546.
3. Kandori, H., Shichida, Y., and Yoshizawa, T. (2001) Photoisomerization in rhodopsin, *Biochemistry (Moscow) 66*, 1197−1209.
4. Okada, T., Ernst, O. P., Palczewski, K., and Hofmann, K. P. (2001) Activation of rhodopsin: New insights from structural and biochemical studies, *Trends Biochem. Sci. 26*, 318−324.
5. Gordeliy, V. I., Labahn, J., Moukhametzianov, R., Efremov, R., Granzin, J., Schlesinger, R., Buldt, G., Savopol, T., Scheidig, A. J., Klare, J. P., and Engelhard, M. (2002) Molecular basis of transmembrane signalling by sensory rhodopsin II-transducer complex, *Nature 419*, 484−487.
6. Sudo, Y., Kandori, H., and Kamo, N. (2004) Molecular mechanism of protein−protein interaction of *pharaonis* phoborhodopsin/transducer and photo-signal transfer reaction by the complex, *Recent Res. Dev. Biophys. 3*, 1−16.
7. Falke, J. J., Bass, R. B., Butler, S. L., Chervitz, S. A., and Danielson, M. A. (1997) The two-component signaling pathway of bacterial chemotaxis: A molecular view of signal transduction by receptors, kinases, and adaptation enzymes, *Annu. Rev. Cell Dev. Biol. 13*, 457−512.

8. Shichida, Y., and Imai, H. (1998) Visual pigment: G-protein-coupled receptor for light signals, *Cell. Mol. Life Sci. 54*, 1299−1315.
9. Sakmar, T. P. (2002) Structure of rhodopsin and the superfamily of seven-helical receptors: The same and not the same, *Curr. Opin. Cell Biol. 14*, 189−195.
10. Helmreich, E. J. M., and Hofmann, K. P. (1996) Structure and function of proteins in G-protein-coupled signal transfer, *Biochim. Biophys. Acta 1286*, 285−322.
11. Royant, A., Nollert, P., Edman, K., Neutze, R., Landau, E. M., Pebay-Peyroula, E., and Navarro, J. (2001) X-ray structure of sensory rhodopsin II at 2.1-Å resolution, *Proc. Natl. Acad. Sci. U.S.A. 98*, 10131−10136.
12. Luecke, H., Schobert, B., Lanyi, J. K., Spudich, E. N., and Spudich, J. L. (2001) Crystal structure of sensory rhodopsin II at 2.4 Å: Insights into color tuning and transducer interaction, *Science 293*, 1499−1503.
13. Palczewski, K., Kumasaka, T., Hori, T., Behnke, C. A., Motoshima, H., Fox, B. A., Le Trong, I., Teller, D. C., Okada, T., Stenkamp, R. E., Yamamoto, M., and Miyano, M. (2000) Crystal structure of rhodopsin: A G protein-coupled receptor, *Science 289*, 739−745.
14. Lambright, D. G., Sondek, J., Bohm, A., Skiba, N. P., Hamm, H. E., and Sigler, P. B. (1996) The 2.0 Å crystal structure of a heterotrimeric G protein, *Nature 379*, 311−319.
15. Nishimura, S., Sasaki, J., Kandori, H., Matsuda, T., Fukada, Y., and Maeda, A. (1996) Structural changes in the peptide backbone in complex formation between activated rhodopsin and transducin studied by FTIR spectroscopy, *Biochemistry 35*, 13267−13271.
16. Nishimura, S., Kandori, H., and Maeda, A. (1998) Interaction between photoactivated rhodopsin and the C-terminal peptide of transducin α-subunit studied by FTIR spectroscopy, *Biochemistry 37*, 15816−15824.
17. Bartl, F., Ritter, E., and Hofmann, K. P. (2000) FTIR spectroscopy of complexes formed between metarhodopsin II and C-terminal peptides from the G-protein α- and γ-subunits, *FEBS Lett. 473*, 259−264.
18. Fahmy, K. (1998) Binding of transducin and transducin-derived peptides to rhodopsin studies by attenuated total reflection-Fourier transform infrared difference spectroscopy, *Biophys. J. 75*, 1306−1318.
19. Furutani, Y., Sudo, Y., Kamo, N., and Kandori, H. (2003) FTIR spectroscopy of the complex between *pharaonis* phoborhodopsin and its transducer protein, *Biochemistry 42*, 4837−4842.
20. Sudo, Y., Furutani, Y., Shimono, K., Kamo, N., and Kandori, H. (2003) Hydrogen bonding alteration of Thr-204 in the complex between *pharaonis* phoborhodopsin and its transducer protein, *Biochemistry 42*, 14166−14172.
21. Sudo, Y., Iwamoto, M., Shimono, K., and Kamo, N. (2001) *pharaonis* phoborhodopsin binds to its cognate truncated transducer even in the presence of a detergent with a 1:1 stoichiometry, *Photochem. Photobiol. 74*, 489−494.
22. Klare, J. P., Gordeliy, V. I., Labahn, J., Buldt, G., Steinhoff, H. J., and Engelhard, M. (2004) The archaeal sensory rhodopsin II/transducer complex: A model for transmembrane signal transfer, *FEBS Lett. 564*, 219−224.
23. Wegener, A. A., Chizhov, I., Engelhard, M., and Steinhoff, H. J. (2000) Time-resolved detection of transient movement of helix F in spin-labelled *pharaonis* sensory rhodopsin II, *J. Mol. Biol. 301*, 881−891.
24. Wegener, A. A., Klare, J. P., Engelhard, M., and Steinhoff, H. J. (2001) Structural insights into the early steps of receptor-transducer signal transfer in archaeal phototaxis, *EMBO J. 20*, 5312−5319.
25. Sudo, Y., Yamabi, M., Iwamoto, M., Shimono, K., and Kamo, N. (2003) Interaction of *Natronobacterium pharaonis* phoborhodopsin (sensory rhodopsin II) with its cognate transducer probed by increase in the thermal stability, *Photochem. Photobiol. 78*, 511−516.
26. Furutani, Y., Iwamoto, M., Shimono, K., Wada, A., Ito, M., Kamo, N., and Kandori, H. (2004) FTIR spectroscopy of the O photointermediate in *pharaonis* phoborhodopsin, *Biochemistry 43*, 5204−5212.
27. Furutani, Y., Iwamoto, M., Shimono, K., Kamo, N., and Kandori, H. (2002) FTIR spectroscopy of the M photointermediate in *pharaonis* rhoborhodopsin, *Biophys. J. 83*, 3482−3489.
28. Engelhard, M., Scharf, B., and Siebert, F. (1996) Protonation changes during the photocycle of sensory rhodopsin II from *Natronobacterium pharaonis*, *FEBS Lett. 395*, 195−198.
29. Bergo, V., Spudich, E. N., Spudich, J. L., and Rothschild, K. J. (2003) Conformational changes detected in a sensory rhodopsin II-transducer complex, *J. Biol. Chem. 278*, 36556−36562.
30. Sudo, Y., Iwamoto, M., Shimono, K., and Kamo, N. (2002) Tyr-199 and charged residues of *pharaonis* phoborhodopsin are important for the interaction with its transducer, *Biophys. J. 83*, 427−432.
31. Steinhoff, H., Savitsky, A., Wegener, C., Pfeiffer, M., Plato, M., and Mobius, K. (2000) High-field EPR studies of the structure and conformational changes of site-directed spin labeled bacteriorhodopsin, *Biochim. Biophys. Acta 1457*, 253−262.
32. Ottemann, K. M., Xiao, W., Shin, Y. K., and Koshland, D. E., Jr. (1999) A piston model for transmembrane signaling of the aspartate receptor, *Science 285*, 1751−1754.

BI047893I